

Effect of oxygen adsorption on the electronic properties of Li/MO₂ (M= Ti, V, Mn) surfaces

Percy Ngobeni, Phuti Ngoepe and Khomotso Maenetja

Material Modelling Centre, University of Limpopo, Private Bag x1106, Sovenga, 0727, South Africa.

Email: percy.ngobeni@ul.ac.za

Abstract: Lithium-air batteries, based on their high theoretical specific energy, are a particularly attractive technology for electrical energy storage. However, they suffer from the production of unstable discharge products which leads to capacity fading of the battery. Several catalysts have been used to improve Oxygen Reduction Reaction (ORR) and Oxygen Evolution Reaction (OER) which will yield stable discharge product. In this study, Density functional theory (DFT) is employed to investigate the relative stability of electronic properties of oxygen adsorption on Li/MO₂ (110) surfaces. Electronic properties such as band structures and density of states (DOS) are investigated on different configurations (dissociated, peroxy on Li, peroxy on Li-M, and peroxy on M) as oxygen is adsorbed on Li/MO₂. The electronic band structures were calculated to check the conductivity of the systems. The DOS was calculated to check the stability of the system by comparing how each system behaves along the Fermi level. These findings are important in improving the cycling performance of Li-air batteries and give insight into the reactivity of Li/MO₂ (110) surfaces.

1. Introduction

Metal-air batteries offer advantageous properties, such as high hypothetical energy and control densities, low working temperature, low cost, and fabric recyclability [1]. Lithium-air batteries are seen by numerous researchers as a potential next-generation innovation in energy capacity with the most elevated hypothetical energy density of all battery devices. The permeable cathode helps with the dissemination of O₂ gas so that it can be transported to the electrolyte-electrode interface as much as conceivable from the lithium-air battery. Li-air is based on either aqueous or nonaqueous electrolyte for which the negative anode is lithium metal, and the positive anode comprises porous carbon as a catalyst [2].

Various studies have employed metal oxides as catalyst for Li-air batteries [3,4]. Transition metal oxides such as MnO₂ has been considered as potential electrocatalysts for bi-functional oxygen terminals due to their high catalytic activity and uncommon disintegration stability for Li-air batteries [5]. The previous study gives insights in understanding charge transfer responses that create the potential distinction within the battery from the Li adatom to the surface M (Mn, Ti, and V) to have lithium-air batteries that are productive [6]. The surface free energies for the most stable composition for the oxidation on the lithiated surfaces of the metal oxides (MnO₂, TiO₂, VO₂) are calculated for different configurations. The oxygen adsorption is examined though in this study we utilize the examined oxygen adsorption on the Li/MO₂ to check the electronic stability of all produced configurations.

2. Methodology

The oxygen adsorption of the Li/MO₂ (110) calculations were performed utilizing the density functional theory (DFT) within the generalized gradient approximation (GGA) utilizing the Perdew, Barker, and Ernzerhof (PBE) exchange-correlation functional [7]. The number of plane waves was chosen by the cut-off kinetic energy of 500 eV and the Brillouin zone examining a plan of Monkhorst-Pack with 6x6x1 k-points work was utilized for the integration inside the reciprocal space for all the (110) surfaces. From the surface calculations the number of k-points was adapted to achieve a similar sampling density in a reciprocal space. Gaussian smearing with a width of 0.05 eV was utilized to progress the convergence amid geometry optimizations.

3. Results and discussion

3.1. Electronic properties overview

The number of states at each energy level, which are accessible to be occupied, is called the density of states (DOS). A zero DOS of an energy level suggests that no states can be possessed. It could be a valuable numerical concept permitting integration about the electron energy to be utilized rather than the integration over the Brillouin zone. Furthermore, the DOS is regularly utilized for quick visual investigation of the electronic structure. The closest band over the bandgap is called the conduction band, and the closest band below the bandgap is called the valence band [8]. In metal or semimetals, the Fermi level is inside of one or more allowed bands. In semimetals, the groups are commonly referred to as "conduction band" or "valence band" depending on whether the charge transport is more electron-like or hole-like, by closeness to semiconductors. In different metals, the bunches are not one or the other electron-like nor hole-like and are frequently sensibly called "valence bunches" as they are made of valence orbitals [9].

3.2. Electronic band structures

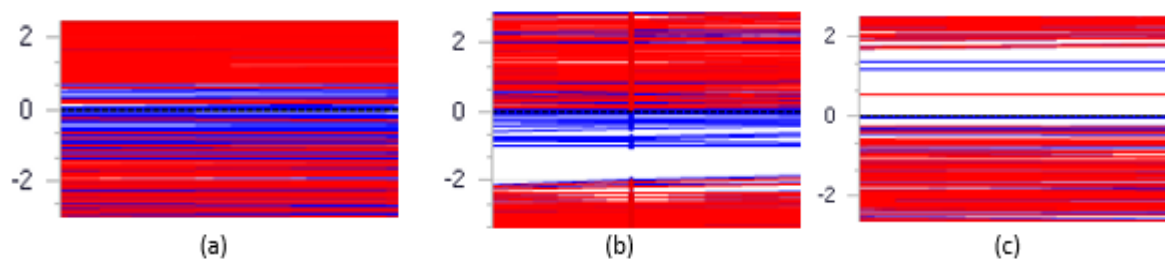


Figure 1. Electronic band structures of (a) (LiMn₄O₉)₄, (b) (LiV₄O₉)₄, and (c) (LiTi₄O₉)₄ dissociated surfaces.

The calculated band structure for (LiMn₄O₉)₄ and (LiTi₄O₉)₄ reveals the presence of a direct gap of 0.007 eV and 0.547 eV respectively, which signifies that the systems are semiconductors. However, there is an absence of an electronic band gap for (LiV₄O₉)₄ at the Fermi level thus the structure is metallic.

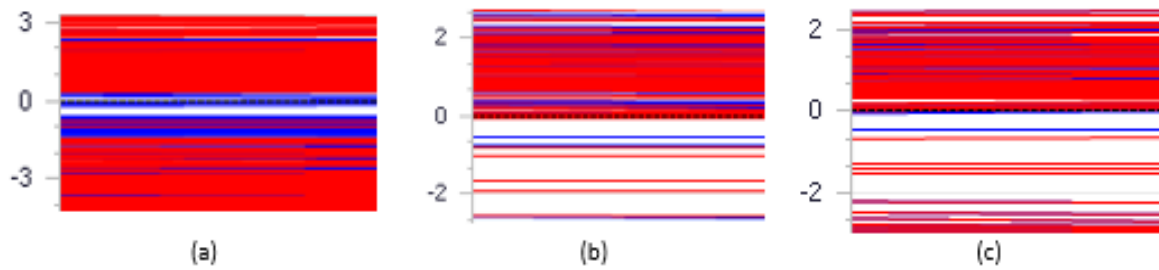


Figure 2. Electronic band structures of (a) $(\text{LiMn}_4\text{O}_9)_4$, (b) $(\text{LiV}_4\text{O}_9)_4$, and (c) $(\text{LiTi}_4\text{O}_9)_4$ peroxo on Li.

The calculated electronic band structures from all the systems $(\text{LiMn}_4\text{O}_9)_4$, $(\text{LiTi}_4\text{O}_9)_4$, and $(\text{LiV}_4\text{O}_9)_4$ affirm a nonappearance of a gap at the Fermi level. Consequently, all the systems are metallic.

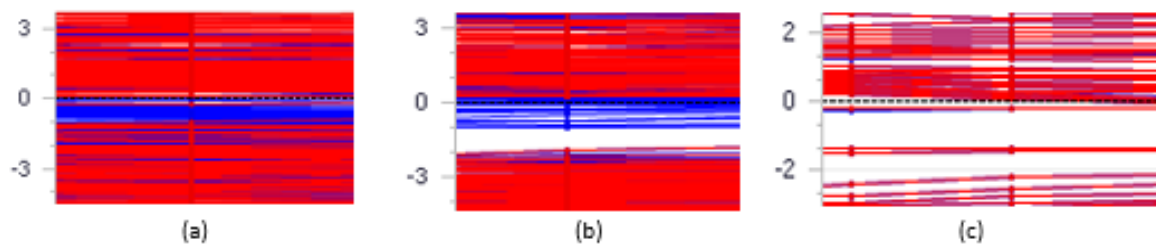


Figure 3. Electronic band structures of (a) $(\text{LiMn}_4\text{O}_9)_4$, (b) $(\text{LiV}_4\text{O}_9)_4$, and (c) $(\text{LiTi}_4\text{O}_9)_4$ peroxo on Li-M.

The calculated electronic band structures from all the systems $(\text{LiMn}_4\text{O}_9)_4$, $(\text{LiTi}_4\text{O}_9)_4$, and $(\text{LiV}_4\text{O}_9)_4$ validates an absence of a gap at the Fermi level. Subsequently, all the systems are metallic.

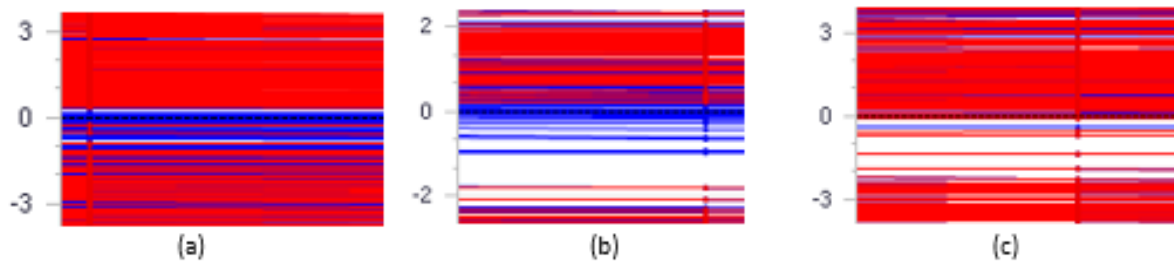


Figure 4. Electronic band structures of (a) $(\text{LiMn}_4\text{O}_9)_4$, (b) $(\text{LiV}_4\text{O}_9)_4$, and (c) $(\text{LiTi}_4\text{O}_9)_4$ peroxo on M.

The calculated band structure for $(\text{LiMn}_8\text{O}_{16})_4$ illustrates the presence of a direct gap at the Fermi level of about 0.035 eV, as a result, the system is a semiconductor. Moreover, there is a nonappearance of an electronic bandgap at the Fermi level for both $(\text{LiTi}_8\text{O}_{16})_4$ and $(\text{LiV}_8\text{O}_{16})_4$ thus the systems are metallic.

The focus of the band structure shown above is mainly at the Fermi level, and other gaps outside the Fermi level are not considered. The conductivity of the material was determined based on the interaction of electron orbitals at the Fermi level. Systems obtained with metallic behavior displayed orbital overlap at the Fermi level, but systems with bandgap less than 3 eV near the Fermi level have been established as semiconductors.

3.3. Density of states (DOS)

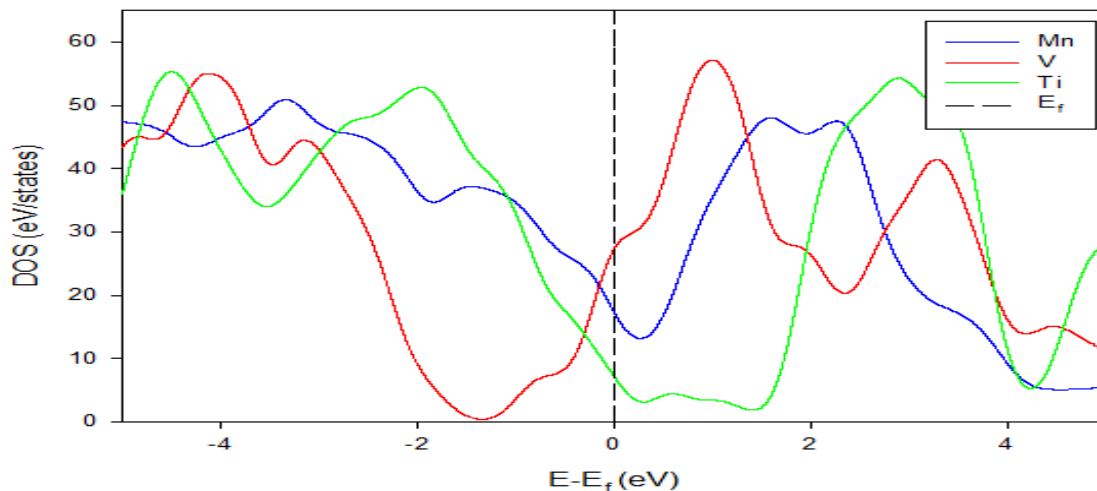


Figure 5. Comparison of the total density of states for the dissociated surfaces.

From figure 5, we observe that near E_f the DOS peak of $(\text{LiV}_4\text{O}_9)_4$ has a higher DOS which suggest the least stability of the system. However, $(\text{LiTi}_4\text{O}_9)_4$ has a lower density of states compared to the other structures near E_f . It is clear that $(\text{LiTi}_4\text{O}_9)_4$ is the most stable compared to $(\text{LiV}_4\text{O}_9)_4$ and $(\text{LiMn}_4\text{O}_9)_4$, the stability trend can be written as $(\text{LiTi}_4\text{O}_9)_4 > (\text{LiMn}_4\text{O}_9)_4 > (\text{LiV}_4\text{O}_9)_4$. However, low Fermi energy for $(\text{LiTi}_4\text{O}_9)_4$ and $(\text{LiMn}_4\text{O}_9)_4$ has been concluded to have a lower catalytic effect for Li-air batteries, since both systems has low number of DOS at the Fermi level.

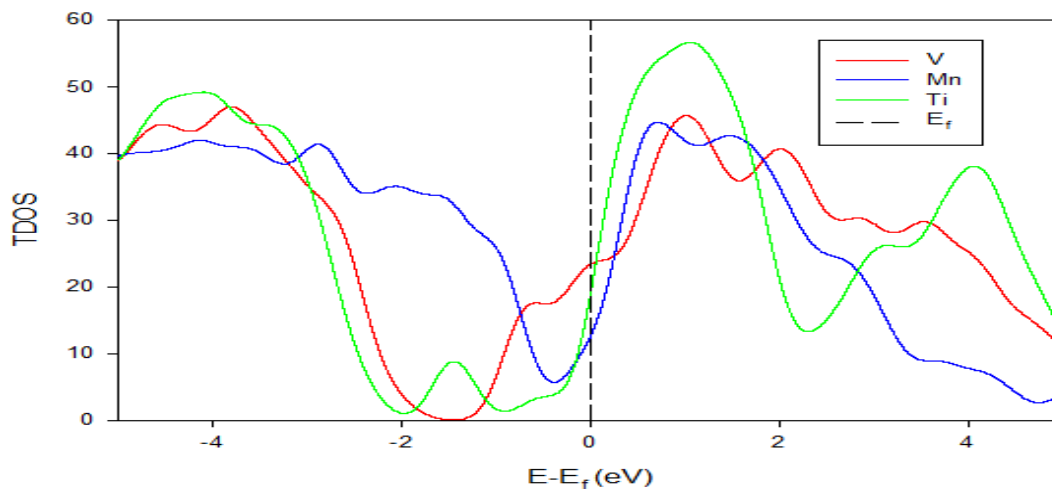


Figure 6. Comparison of the overall density of states for the Peroxo on Li surfaces.

Figure 6 shows the total density of states (TDOS) for $(\text{LiMn}_4\text{O}_9)_4$, $(\text{LiTi}_4\text{O}_9)_4$, and $(\text{LiV}_4\text{O}_9)_4$ surfaces. We notice that towards E_f the DOS peak of $(\text{LiMn}_4\text{O}_9)_4$ has a lower density of states which agrees that it is the most stable structure. Furthermore, we notice that $(\text{LiTi}_4\text{O}_9)_4$ and $(\text{LiV}_4\text{O}_9)_4$, both have a higher density of states at E_f compared to $(\text{LiMn}_4\text{O}_9)_4$. The DOS for $(\text{LiV}_4\text{O}_9)_4$ has a higher density of states at E_f , indicating that it is the least stable structure. The stability trend can be written as $(\text{LiMn}_4\text{O}_9)_4 > (\text{LiTi}_4\text{O}_9)_4 > (\text{LiV}_4\text{O}_9)_4$. In any case, low Fermi energy for $(\text{LiTi}_4\text{O}_9)_4$ and $(\text{LiMn}_4\text{O}_9)_4$ has been concluded to have a lower catalytic impact for Li-air batteries.

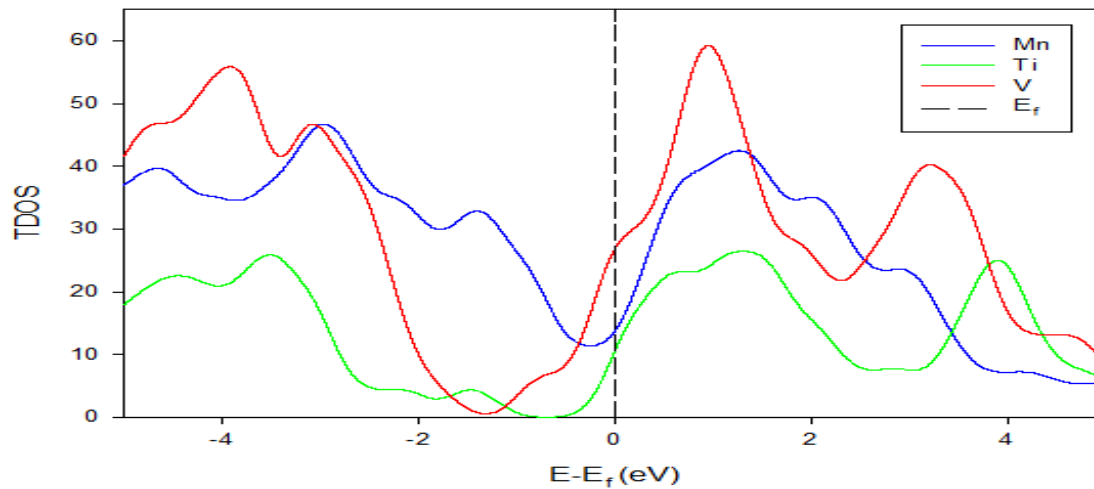


Figure 7. Comparison of the full density of states for Peroxo on Li-M surfaces.

The total density of states (TDOS) for $(\text{LiMn}_4\text{O}_9)_4$, $(\text{LiTi}_4\text{O}_9)_4$, and $(\text{LiV}_4\text{O}_9)_4$ surfaces is observed above in figure 7. We notice that along with E_f the DOS peak of $(\text{LiMn}_4\text{O}_9)_4$ has a lower density of states which agrees that it is the most stable structure with a slight shift towards the conduction band. Furthermore, we notice that $(\text{LiTi}_4\text{O}_9)_4$ and $(\text{LiV}_4\text{O}_9)_4$, both have a higher density of states at E_f compared to $(\text{LiMn}_4\text{O}_9)_4$. The shift from the valence band from both $(\text{LiTi}_4\text{O}_9)_4$ and $(\text{LiV}_4\text{O}_9)_4$ to the conduction band is observed. The DOS for $(\text{LiV}_4\text{O}_9)_4$ has a higher density of states at E_f , indicating that it is the least stable structure. The stability trend can be written as $(\text{LiMn}_4\text{O}_9)_4 > (\text{LiTi}_4\text{O}_9)_4 > (\text{LiV}_4\text{O}_9)_4$. However, low Fermi energy for $(\text{LiTi}_4\text{O}_9)_4$ and $(\text{LiMn}_4\text{O}_9)_4$ has been concluded to have a lower catalytic impact for Li-air batteries.

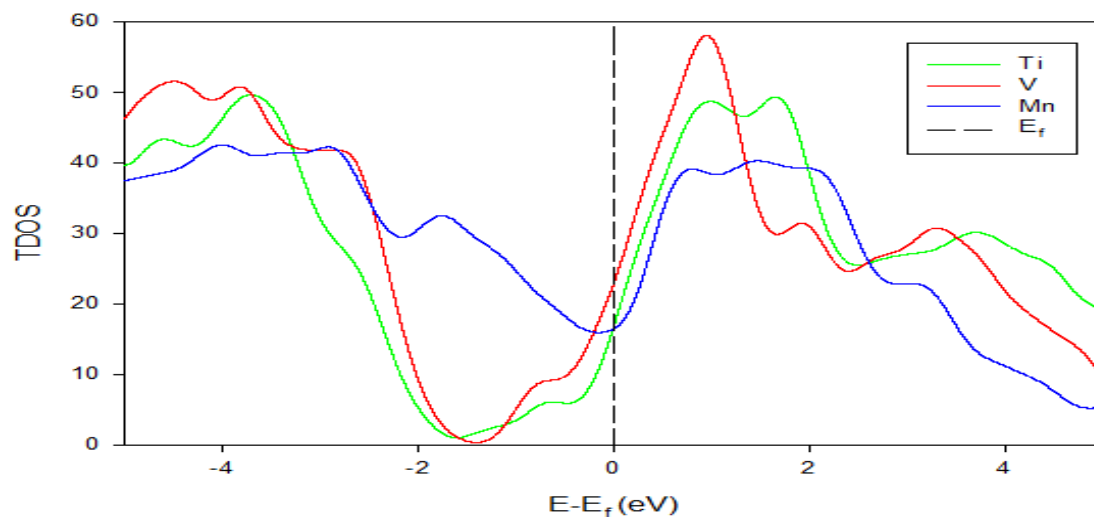


Figure 8. Comparison of the overall density of states for the Peroxo on M surfaces.

The total density of states (TDOS) for $(\text{LiMn}_4\text{O}_9)_4$, $(\text{LiTi}_4\text{O}_9)_4$, and $(\text{LiV}_4\text{O}_9)_4$ surfaces is displayed in figure 8 above. We note that near E_f the DOS peak of $(\text{LiMn}_4\text{O}_9)_4$ has a lower density of states which agrees that it is the most stable. However, we notice that $(\text{LiTi}_4\text{O}_9)_4$ and $(\text{LiV}_4\text{O}_9)_4$, both have higher density of states at E_f compared to $(\text{LiMn}_4\text{O}_9)_4$. The shift from the valence band from both $(\text{LiTi}_4\text{O}_9)_4$ and $(\text{LiV}_4\text{O}_9)_4$ to the conduction band is observed. The DOS for $(\text{LiV}_4\text{O}_9)_4$ has a higher density of states at E_f , suggesting that it is the least stable structure. The stability trend can be written as $(\text{LiMn}_4\text{O}_9)_4 >$

$(\text{LiTi}_4\text{O}_9)_4 > (\text{LiV}_4\text{O}_9)_4$. However, low Fermi energy for $(\text{LiTi}_4\text{O}_9)_4$ and $(\text{LiMn}_4\text{O}_9)_4$ has been concluded to have a lower catalytic impact for Li-air batteries.

After successful adsorption with oxygen at the Li/MO₂, there are arrangements produced (dissociated, peroxy on Li, peroxy on Li-M, and peroxy on M). Configurations such as peroxy on Li, peroxy on Li-M, and peroxy on M yielded the same trend of stability when observing the density of states with $(\text{LiMn}_4\text{O}_9)_4$ found to have less density of states at the Fermi level in all arrangements obtained, followed by the $(\text{LiTi}_4\text{O}_9)_4$ frameworks. The final one from the observed results is $(\text{LiV}_4\text{O}_9)_4$ with a high density of states at the Fermi level, the electronic band structures compare well with the density of states. The behavior of the frameworks is characterized by how the frameworks are associated with the Fermi level, which ordinarily results in finding a way of classifying the metallic, semiconductor, and insulator behavior.

4. Conclusion

The electronic properties were effectively obtained from the DFT using the Vasp and CASTEP codes. The k-points used throughout the calculations are 6x6x1 for all the (110) surface systems. The electronic properties such as the electronic band structures and the density of states were successfully obtained for the clean (110) surfaces. Oxygen adsorption on the Li/MO₂ resulted in configurations such as the dissociated, peroxy on Li, peroxy on Li-M, and peroxy on M. The stability of these specified arrangements was distinguished by how much contribution each system makes to the Fermi level. The high density of states means the system is less stable compared to the one with a low density of states at the Fermi level. However, from all the configurations mentioned above $(\text{LiTi}_4\text{O}_9)_4$ and $(\text{LiMn}_4\text{O}_9)_4$ are found to have lower catalytic impact due to low Fermi energy contributions. The electronic band structures compared well with the energy of states. These discoveries are critical in progressing the cycling execution of Li-air batteries and provide understanding into the reactivity of Li/MO₂ (110) surfaces.

5. References

- [1] Tahir M, Pan L, Idrees F, Zhang X, Wang L, Zou J, and Wang Z L 2017 Electrocatalytic oxygen evolution reaction for energy conversion and storage: A comprehensive review *Nano Energy* **37** 126-157
- [2] Cheong K Y, Impellizzeri G, and Fraga M A 2018 Emerging materials for energy conversion and storage *Elsevier*
- [3] Geng D, Ding N, Andy Hor T S, Chien S W, Liu Z, Wu D, Sun X, and Zong Y 2016 From Lithium-Oxygen to Lithium-Air Batteries: Challenges and opportunities *Adv. Energy Mater.* **9** 1502164
- [4] Bruce P G, Freunberger S A, Hardwick L J and Tarascon J M 2012 Li-O₂ and Li-S batteries with high energy storage *Nature Materials*. **11** 19-29
- [5] Li Q, Cao R, Cho J and Wu G 2014 High-Performance Direct Methanol Fuel Cells with Precious-Metal-Free Cathode *Phys. Chem. Chem. Phys.* **16** 13568
- [6] Maenetja K P 2017 Density functional theory study of (110) β -MnO₂, β -TiO₂ and β -VO₂ surface in metal-air batteries *Unive of Limp thesis*
- [7] Abrahams S C and Bernstein J L 1971 Rutile: Normal Probability Plot Analysis and Accurate Measurement of Crystal Structure *Chem. Phys.* **55** 3206
- [8] Du X, Huang J, Zhang J, Yan Y, Wu C, Hu Y, Yan C, Lei T, Chen W, Fan C, and Xiong J 2018 Modulating Electronic Structures of Inorganic Nanomaterials for Efficient Electrocatalytic Water Splitting *A Journal of the German chemical society* **58** 4484-4502
- [9] Choy T S, Naset J, Chen J, Hershfield S, and Stanton C 2000 A data of Fermi surface in virtual reality modelling language (VRML) *Bull. Amer. Phys. Soc.* **45** 36-42